INVESTIGATION OF WOOD IMPACT PROPERTIES USING FRACTAL DIMENSION ANALYSIS

Shaoqun Zhang
Associate Professor
E-mail: junyang580@sohu.com

*Jun Hua**†*
Professor
E-mail: huajun81@163.com

Wei Xu
Research Assistant
E-mail: hljhrbxw@163.com

Guangwei Chen
Associate Professor
College of Electromechanical Engineering
Northeast Forestry University
Harbin 150040, PR China
E-mail: gladiator429@aliyun.com

Sheldon Q. Shi†
Associate Professor
E-mail: Sheldon.Shi@unt.edu

Liping Cai
Researcher
Mechanical and Energy Engineering Department
University of North Texas
Denton, TX
E-mail: Liping.Cai@unt.edu

(Received March 2014)

Abstract. Fractal analysis is a research tool recently used to model various processes. However, this analysis has not been used for determining impact properties of wood. In this study, the transverse and longitudinal impact ductility of five species, ie white pine, poplar, pine, birch, and basswood, was experimentally determined. Based on the grid-cover method, photographs were taken of the fracture surfaces and edited by image graying using Photoshop CS5 (Adobe Systems Inc.). The yardstick δ was determined by adjusting the distance between the grid lines. The slope K of the regression equation of $\text{Log}(1/\delta_i)$ vs $\text{Log}(N[\delta_i])$ was the fractal dimension D_L of the fracture profile curve. Fractal dimension allows us to measure the complexity of fracture profiles after the specimens were broken by impacts. The results indicate that the average fractal dimension values were 2.023-2.075 on the fractures from transverse and longitudinal impacts. The longitudinal impact ductility was greater than the transverse for all tested species. The transverse and longitudinal impact ductility was linearly related to the fracture fractal dimension.

Keywords: Fractal dimension, impact ductility, transverse and longitudinal directions, regression.

* Corresponding author
† SWST member

INTRODUCTION

As is well known, the dimensions of a line, a square, and a cube are one, two, and three, respectively. The distance, area, and volume of those objects are measurable as well. However, what is the dimension of the inside of a kidney or the fracture surfaces when a specimen is broken, and how do we measure their surface area? Fractal dimension allows us to measure the complexity of an object. The fractal dimension is able to provide a wealth of information about the shape of a fracture, the fracture energy, the toughness of material, and many other related properties. The concept of fractal geometry is much more general and allows finding more general relations between the structure of materials and physical phenomena. Numerous studies regarding metal performances have been completed in the past (Underwood and Baner 1986). The fractal data were obtained from the fracture surfaces and their profiles. The physical nature of the fractal dimension was afforded by its close similarity to fracture roughness parameters that had simple physical meanings. To check for "self-similitude" of any irregular nature curve, the linearity of the entire fractal plot was examined (Underwood 1994).

The fractal dimensions of metallic fracture surfaces were examined by Kotowski (2006), which included the influences of the mechanical notch radius in a compact specimen on the fractal dimension of the fracture surface, the distortion rate on the fractal dimension, the fatigue crack propagation rate on the fractal dimension, and the stress-intensity factor on the fractal dimension of the fracture surface. The occurrence of fracture processes from images of fractures in specimens of molybdenum and porous iron was investigated based on the approaches of fractal geometry (Trefilov et al 2001).

Some studies reported applications of fractal models in porous media and porous materials. Based on the thermal–electrical analogy and statistical self-similarity of porous media, a fractal analysis of effective thermal conductivity for unsaturated fractal porous media was developed by Kou et al (2009). With a dimensionless expression of effective thermal conductivity, the effect of the parameters of fractal porous media on the dimensionless effective thermal conductivity was explored. The effect of the fractal dimension of a fracture surface and spall contour on the characteristics of the loaded material was investigated by Barakhtin and Savenkov (2009). The results showed that an increase in the fractal dimensions of the spall contour led to an increase in the material strength parameter in the tensile wave and spall strength, whereas an increase in the fractal dimension of the fracture surface decreased the spall strength.

The fractal dimension was a more appropriate measure than the average surface roughness for evaluation of the adhesion strength of ceramic coatings (Amada and Satoh 2000). The adhesion strength of plasma-sprayed ceramic coatings was affected by surfaces roughened by grit blasting. Because of the fractal characteristics on the blasted surface, the surface topography of substrates was evaluated using fractal analysis.

Limited studies regarding the applications of fractal analysis in wooden materials were carried out. The actual cracked wood surface induced by a crack extension was described using a fractal pattern by Morel and Valentin (1999). The roughening led to R-curve behavior whereas the fracture toughness, K_R, depended on the crack length increment $\triangle a$ as a power law K_R-$\triangle a^{(\zeta\text{-}\zeta loc)/2z}$ characterized by the exponents of the scaling properties (ζ and ζ_{loc} are the global and local roughness exponents and z is the dynamic exponent). The link between morphology of fracture surface and fracture toughness also provided a size effect on the critical resistance K_{RC}. In terms of energy, the critical energy release rate, G_{RC}, depended on the specimen size as a power law G_{RC} - $L^{\zeta\text{-}\zeta loc}$. Predicted results were confirmed by comparison with fracture experiments on Norway spruce and Maritime pine.

The relationship between the fractal dimension of wood anatomy structure and impact energy was reported by Konas et al (2009). A slight modification of common methods for experimental

evaluation of fractal dimensions was performed, which can be used as an interesting alternative to estimate mechanical properties of wood without using destructive experimental tests. The comparison of relation significance of impact energy and linear combination of those fractal dimensions was carried out. In contrast to the common way of estimating the relation between impact energy and fractal dimension of fracture after impact loading, a sufficient amount of information about toughness in the original state (before loading) was provided for the estimation. Because of the complicated experimental assessment of toughness, the work of impact loading as a measurable magnitude of material toughness was used.

Using X-ray computed tomography images and a computer image processing technique, the fractal dimensions of void size (FDVS) in oriented strandboard were investigated by Li et al (2013). The FDVS value was high in the panel surface layers and decreased toward the panel center. Although there are questions regarding this finding, it is a good introduction of fractal theory to wood-based composites.

This study aimed at investigating wood impact properties using fractal dimension analysis. This dimension was determined for the vertical profile obtained by the profile technique with a camera and edited using the image graying method. By examining the fractal dimension values on the fractures from transverse and longitudinal impacts, the relationship between the impact ductility and the fracture fractal dimension could be established.

FRACTAL THEORY AND TEST METHODS

One of the common methods for determining the fractal dimension of fracture of materials is to measure the vertical profile (Underwood and Baner 1986; Underwood 1994). As shown in Fig 1, A_0 and L_0 are the projective geometer of fracture surface A and surface vertical profile contour line length L, respectively. When the profile line L was measured by yardstick δ and

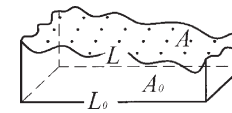

Figure 1. Fracture surface of failure.

the fracture surface was measured by area measure ε, the arrived equation is as follows:

$$A(\varepsilon) = A_0\varepsilon^{2-D_A} \tag{1}$$

The relationship between the fractal surface vertical profile line L and its projective geometer is

$$L(\delta) = L_0\delta^{1-D_L} \tag{2}$$

where D_L is the fractal dimension of the surface vertical profile line, which can be obtained by calculating the electronically scanned curve using the grid-cover method. The roughness of the actual profile line is $R_L = L(\delta)/L_0$. Similarly, the roughness of the fracture surface can be described as $R_A = A(\varepsilon)/A_0$. The relationship between R_A and R_L is (Underwood and Baner 1986; Underwood 1994)

$$R_A = \frac{4}{\pi}(R_L - 1) + 1 \tag{3}$$

Substituting Eqs 1 and 2 into 3, this becomes

$$\varepsilon^{2-D_A} = \frac{4(\delta^{1-D_L} - 1)}{\pi} + 1 \tag{4}$$

Because the fractal dimension of the fracture surface A and the fractal dimension of profile line L were in the same dimensional range, by assuming $\varepsilon = \delta^2$, the fractal dimension of the fracture surface D_A can be expressed as follows:

$$D_A = \frac{\ln\left[\dfrac{\pi\delta^4}{4(\delta^{1-D_L} - 1) + \pi}\right]}{2\ln\delta} \tag{5}$$

Five species (white pine [*Pinus bungeana* Zuco. exEnd], poplar [*Liriodendron tulipifera*], pine [*Pinus sylvestris*], birch [*Betula papyrifera*], and basswood [*Tiliaceae*]) from Heilongjiang Province, China, were used in this study. Two types of specimens for the two impact directions, ie transversal and longitudinal, were prepared as shown in Fig 2. Before the impact tests,

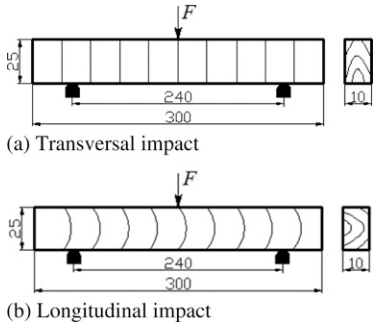

Figure 2. Size of the specimen (mm) and impact directions: (a) transversal impact and (b) longitudinal impact.

all specimens were placed in a conditioning chamber with 70% RH at 20°C for 2 wk. Because different species have different equilibrium moisture contents, different moisture contents were obtained (Table 1). Impact ductility was measured using an MW-4 pendulum impact tester with impact energy up to 21.7 J and an impact velocity of 3.3 m/s. In accordance with Chinese standard GB/T 1929-2009 (Chinese National Standard 2009), test specimens were 300 × 10 × 25 mm (length × width × thickness) (Fig 2). During the fall from its raised position, the pendulum's potential energy decreased, changing into kinetic energy. The kinetic energy was at its greatest just before impact. This was the impact energy. The energy absorbed by the test specimen during failure (ie fracturing or breaking) was determined from the height of the pendulum after impact.

After each impact test, a photograph of the fracture surface was taken and analyzed by a computer. Figure 3 shows the fracture cross-section profile lines and its fractal curves for pine and birch. Impact testing results are presented in Table 1.

IMAGE AND FRACTAL DIMENSION ANALYSIS

When white pine and pine specimens were subjected to a transversal impact, they were broken along the impact direction and the fracture surfaces were relatively smooth (Fig 3a) (the fracture profile contour line of pine). When birch and basswood specimens were subjected to transversal impact, the fracture surfaces crumpled (Fig 3c) (the fracture profile contour line of birch). Because the impact ductility of birch and basswood was 2.7-3.0 times higher than that of pine (Table 1), it was more difficult to break birch and basswood. As a result, uneven fracture surfaces were obtained.

When white pine, poplar, and pine specimens were subjected to a longitudinal impact, they were linearly broken along the impact direction and the fracture surfaces were relatively smooth (Fig 3b) (the fracture profile contour line of pine). When basswood specimens were subjected to a longitudinal impact, the fracture surfaces were smooth. Because of the fine fiber construction of basswood, the fracture surfaces were smoother than those of white pine and pine. When birch specimens were broken by the longitudinal impact, the fracture surfaces were crumpled (Fig 3d). The higher impact ductility of birch (Table 1) made it harder to break, resulting in the jagged fracture surfaces.

According to the grid-cover method, after the specimen was broken, the typical fracture profile curves were selected and photographs of them were taken. With Photoshop CS5 (Adobe Systems, Inc.), these photographs were edited by image graying and the curve was covered by grids. The yardstick δ was determined by

Table 1. Impact ductility of different species.

		White pine		Poplar		Pine		Birch		Basswood	
Species	Sample size	Ave.	SD[a]	Ave.	SD	Ave.	SD	Ave.	SD	Ave.	SD
Density (g/cm^3)	10	0.384	0.063	0.432	0.015	0.461	0.043	0.529	0.040	0.559	0.038
Moisture content (%)	10	14.11	0.033	12.64	0.034	13.10	0.032	11.15	0.025	15.88	0.026
Transversal (kJ/m^2)	10	0.748	0.196	0.897	0.315	0.750	0.235	2.206	0.666	1.994	0.217
Longitudinal (kJ/m^2)	10	0.811	0.278	1.178	0.540	0.980	0.404	3.554	1.018	2.171	0.324

[a] SD, standard deviation.

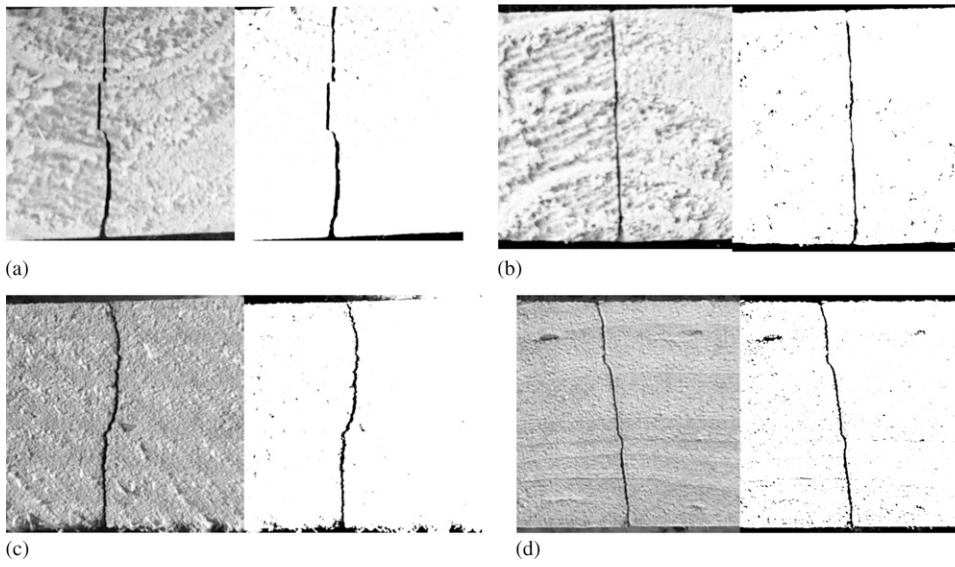

Figure 3. Pine and birch impact fracture photographs and fractal curves: (a) transversal impact fracture profile contour line and fractal curve of pine; (b) longitudinal impact fracture profile contour line and fractal curve of pine; (c) transversal impact fracture profile contour line and fractal curve of birch; (d) longitudinal impact fracture profile contour line and fractal curve of birch.

adjusting the distance between the grid lines (Fig 4).

The yardstick δ was changed by increasing the number of grids (Fig 4b). Because the number $N(\delta)$ of grids with that curve was increased as yardstick δ decreased, a set of varied data $[\delta_i, N(\delta_i)]$ presented. After taking logarithms for $1/\delta_i$ and $N(\delta_i)$, a group of new data set ($\log[1/\delta_i]$, $\log[N\{\delta_i\}]$) was obtained for linear regression. The slope K of the regression equation was the fractal dimension D_L of the fracture profile curve. Figure 5 illustrates the linear regression result for the longitudinal impact of pine.

Figure 5 shows there was an excellent linear relationship between $\log(N[\delta])$ and $\log(1/\delta)$ ($R^2 = 0.998$). There were obvious similarities

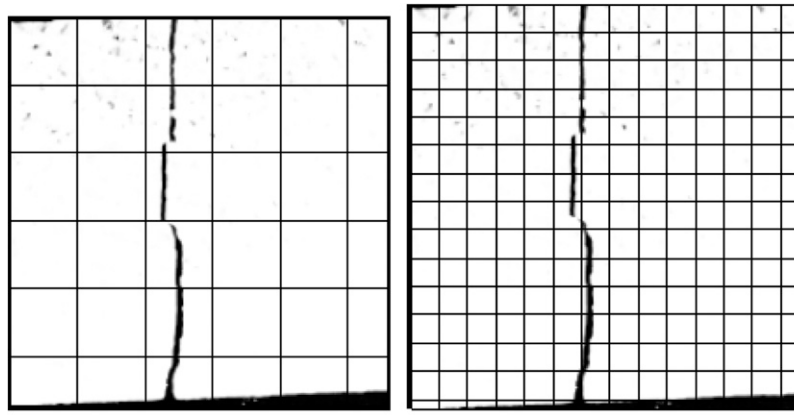

(a) Grids cover the fracture profile curve

(b) Fracture profile curve covered by increasing no. of grids

Figure 4. Grid-cover method for fracture profile curve covered.

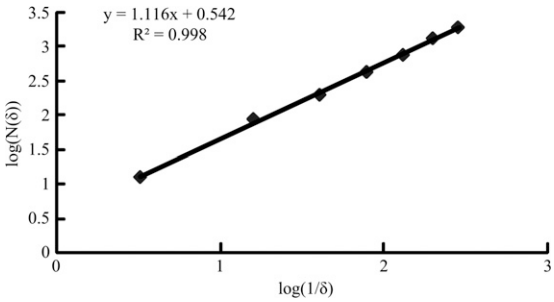

Figure 5. Linear regression for pine.

between the global and local fracture surface profile lines, namely, the profile line-shade fractal fracture characteristics (fractal dimension $D_L = 1.116$). According to Eq 5, fracture surface fractal dimension D_A can be calculated from profile line fractal dimension D_L. The fractured surface fractal dimension $D_A = 2.074$. Using this method, the average fractal dimension for five species and two fracture types are presented in Table 2 (10 replicates).

Table 2 illustrates that the average fractal dimension values ranged from 2.023 to 2.075 for the transverse and longitudinal impact. The difference between the maximum and minimum values was 0.036. In the transversal impact fracture, the greatest fractal dimension was basswood (2.059) and the smallest was birch (2.023). The difference between the maximum and minimum was 0.036. In the longitudinal impact fracture, the largest fractal dimension was poplar (2.075) and the smallest was birch (2.037). The difference between the maximum and minimum was 0.038.

RELATIONSHIP AMONG IMPACT DUCTILITY, DENSITY, AND FRACTURE FRACTAL DIMENSION

Figure 6 shows that the longitudinal impact ductility was greater than that of transversal impact.

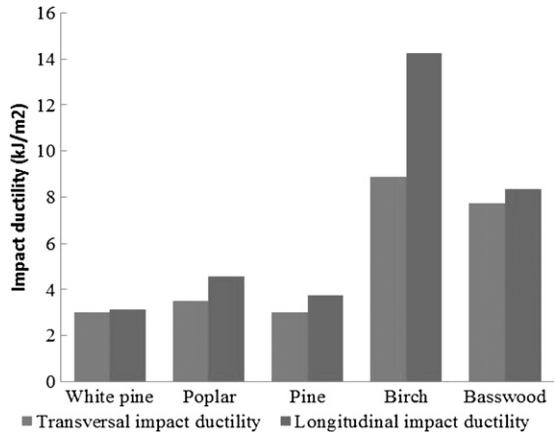

Figure 6. Transversal and longitudinal impact ductility.

The longitudinal impact ductility of white pine, poplar, pine, birch, and basswood was 1.08, 1.31, 1.30, 1.61, and 1.08 times that of the transversal impact, respectively. Considerable differences between the transverse and longitudinal impact ductility for poplar, pine, and birch occurred, whereas relatively small differences for white pine and basswood were found. Because the longitudinal impact ductility was greater than the transverse one, the specimens were more easily broken under transverse impact. An angle of approximately 0° between the impact direction and the fiber direction was noted when the specimens were broken by the transverse impact (Fig 2a) and approximately 30° the specimens were broken by the longitudinal impact (Fig 2b). As is well-known, greater impact force is required to break fibers when the impact angles are greater. This finding agreed well with the one reported by Berg et al (2009). It was indicated that more energy was needed to create cracks with higher microfibril angles.

Furthermore, it could be reasoned that the lignin crosslinks in the longitudinal plane made it stronger than in the transvers plane, which was

Table 2. Average fractal dimension for different species.

		White pine		Poplar		Pine		Birch		Basswood	
Fracture type	Sample size	Ave.	SD[a]	Ave.	SD	Ave.	SD	Ave.	SD	Ave.	SD
Transversal impact	10	2.045	0.005	2.045	0.03	2.03	0.027	2.023	0.014	2.059	0.029
Longitudinal impact	10	2.051	0.011	2.075	0.053	2.067	0.028	2.037	0.013	2.054	0.014

[a] SD, standard deviation.

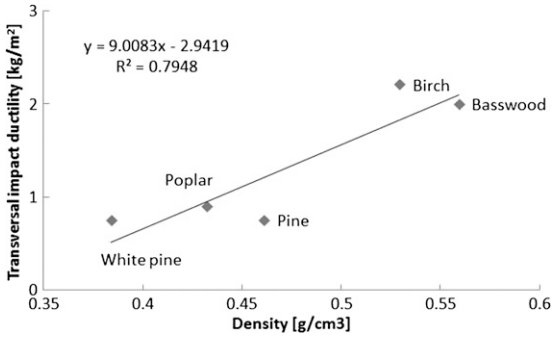

Figure 7. Relationship between transverse impact ductility and density.

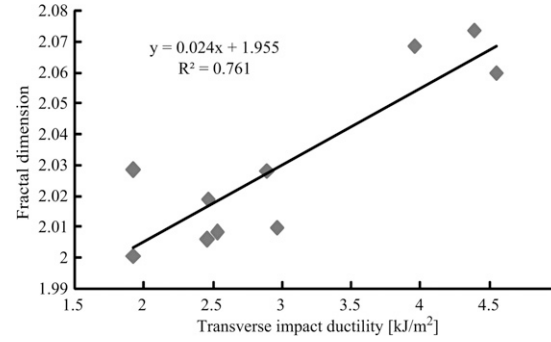

Figure 9. Regression of transverse impact ductility and fractal dimension of pine.

consistent with Zhang et al (2011). It was reported that the cutting forces in the longitudinal direction were higher than those in the transverse direction for Chinese fir, Mongolian pine, and Manchurian ash because of the high complexity of structure in the longitudinal plane that may correspond with higher linking of structural parts on an anatomy scale.

Based on the data in Table 1, regressions for transverse impact ductility and density, longitudinal impact ductility, and density were carried out (Figs 7 and 8). The correlation coefficients R^2 were 0.79 and 0.61, respectively. Wood density plays an essential role on impact ductility because the higher density implies denser wood structure and more cell wall substances in a cubic unit of wood. Wood cell walls are much stronger than lumen or vacuole. Usually, higher density wood leads to higher impact

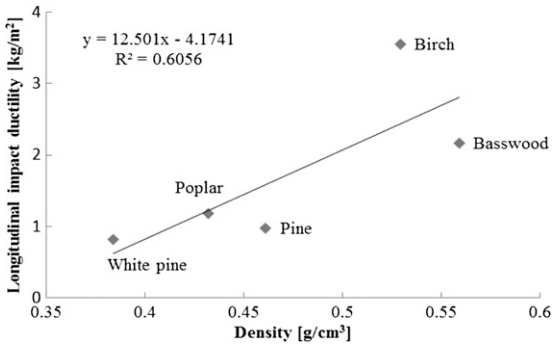

Figure 8. Relationship between longitudinal impact ductility and density.

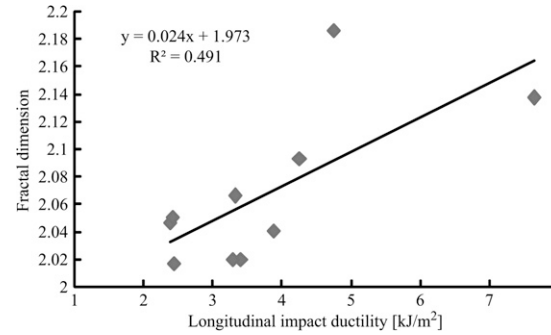

Figure 10. Regression of longitudinal impact ductility and fractal dimension of pine.

ductility for structural timber (Jorissena and Fragiacomo 2011).

The relationships of the transverse and longitudinal impact ductility (Table 1) and the fractal dimension values (Table 2) were analyzed by regression. As examples, the pine regression curve for the transverse impact ductility and the fractal dimension and the pine regression curve for the longitudinal impact ductility and the fractal dimension are illustrated in Figs 9 and 10, respectively. The correlation coefficients R^2 were 0.76 and 0.49, respectively. Thus, the impact ductility of wood can be estimated by the determination of the fracture fractal dimension.

CONCLUSIONS

1. The transverse and longitudinal impact ductility was linearly related to the fracture fractal dimension.

2. Average fractal dimension values ranging from 2.023 to 2.075 occurred on the fractures from transverse and longitudinal impacts. The fractal dimension can be used for predicting the impact ductility of wood.
3. The longitudinal impact ductility was greater than the transverse for all tested species.

ACKNOWLEDGMENTS

This work was supported by the Natural Science Foundation of China (NSFC) through grant number 31070499.

REFERENCES

Amada S, Satoh A (2000) Fractal analysis of surfaces roughened by grit blasting. J Adhes Sci Technol 14(1):27-41.

Barakhtin BK, Savenkov GG (2009) Relationship between spall characteristics and the dimension of fractal fracture structures. J Appl Mech Tech Phys 50(6):965-971.

Berg J-E, Gulliksson ME, Gradin PA (2009) On the energy consumption for crack development in fiber wall in disc refining. Holzforschung 63:204-210.

Chinese National Standard (2009) Chinese Standard GB/T 1929-2009. Method of sample log sawing and test specimen selection for physical and mechanical tests of wood. Beijing, China.

Jorissena A, Fragiacomo M (2011) General notes on ductility in timber structures. Eng Struct 33(11):2987-2997.

Konas P, Buchar J, Severa L (2009) Study of correlation between the fractal dimension of wood anatomy structure and impact energy. Eur J Mech A, Solids 28(5):545-550.

Kotowski P (2006) Fractal dimension of metallic fracture surface. Int J Fract 141(3):269-286.

Kou J, Liu Y, Wu F, Fan J, Lu H, Xu Y (2009) Fractal analysis of effective thermal conductivity for three-phase (unsaturated) porous media. J Appl Physics 106(4):054905.

Li P, Wu Q, Tao Y (2013) Fractal dimension analysis of void size in wood-strand composites based on X-ray computer tomography images. Holzforschung 67(2):177-182.

Morel S, Valentin G (1999) Roughness of wood fracture surfaces and fracture toughness. Pages 13-15 *in* 1st RILEM Symposium on Timber Engineering, L Böstrom, ed, September 1999. RILEM Publications, Stockholm, Sweden.

Trefilov VI, Kartuzov VV, Minakov NV (2001) Fractal dimension of fracture surfaces. Metal Sci Heat Treat 43(3-4):95-98.

Underwood EE (1994) Fractals in materials research. Acta Stereol 13(2):269-276.

Underwood EE, Baner JIA (1986) Fractals in fractography. Mater Sci Eng 80(1):1-14.

Zhang ZK, Peng XR, Li WG, Zeng J, Wang BG (2011) Influence of cutting direction on cutting forces in wood. China Wood Industry 25(6):7-9.